The American Journal of Pathology, Vol. 188, No. 11, November 2018

The American Journal of
PATHOLOGY
ajp.amjpathol.org

GASTROINTESTINAL, HEPATOBILIARY, AND PANCREATIC PATHOLOGY

The Role of Neonatal Gr-1$^+$ Myeloid Cells in a Murine Model of Rhesus-Rotavirus–Induced Biliary Atresia

Ruizhong Zhang,* Zefeng Lin,* Ming Fu,* Xisi Guan,* Jiakang Yu,* Wei Zhong,* Jixiao Zeng,* Vincent C.H. Lui,† Paul K.H. Tam,† Jonathan R. Lamb,‡ Huimin Xia,* and Yan Chen*†

From the Department of Pediatric Surgery, Guangzhou Women and Children's Medical Center, Guangzhou Medical University, Guangzhou, China; the Department of Surgery,† the University of Hong Kong, Hong Kong SAR, China; and the Department of Life Sciences,‡ Faculty of Natural Sciences, Imperial College London, London, United Kingdom*

Accepted for publication July 25, 2018.

Address correspondence to Yan Chen, Ph.D., L9-43, Faculty of Medicine Building, Department of Surgery, The University of Hong Kong, 21, Sassoon Rd., Pokfulam, Hong Kong SAR, P.R. China; or Huimin Xia, M.D., Guangzhou Women and Children's Medical Center, 9 Jinsui Rd., Guangzhou 510623, P.R. China. E-mail: ychenc@hku.hk or xia-huimin@foxmail.com.

Activation of innate immunity together with cholangiocyte damage occurs in biliary atresia (BA). However, detailed information on the inflammatory cells involved is lacking. This study investigates both the pathophysiology of CD11b$^+$Gr-1$^+$ cells in a mouse model of BA and their presence in BA patients. CD11b$^+$Gr-1$^+$ cells were targeted by an anti-Ly6G antibody in murine BA induced by inoculation with rhesus rotavirus. Expression of the Ly6G homolog CD177$^+$ was examined in biopsies from BA patients. The symptoms of BA were ameliorated, and survival was prolonged in those mice receiving 5 to 10 μg of antibody per mouse every 3 days for four times compared with the mice treated with virus alone. However, the mice later developed chronic BA with persistent low body weight and jaundice. Hepatic inflammatory cells were reduced compared with acute BA. Blockade of extrahepatic bile ducts occurred, whereas intrahepatic ductules were partially preserved, and a progressive increase in liver fibrosis was observed. High levels of CD11b$^+$Gr-1$^+$ cells were present in these mice. The administration of an anti-Ly6G antibody again in those chronic BA mice reduced jaundice and restored body weight. In BA patients CD177$^+$ cells were highly expressed in the liver. Our data suggest that the chronic mouse BA model shares key characteristics with clinical BA and indicates the importance of CD11b$^+$Gr-1$^+$ cells in the initiation and progression of BA. *(Am J Pathol 2018, 188: 2617–2628; https://doi.org/10.1016/j.ajpath.2018.07.024)*

Activation of innate immunity is an essential response to microbial infection. However, in newborn infants the situation is different from that of adults because the development of both innate and adaptive immunity is at the initiation stage. Maternally inherited immunity as well as genetic variation and environmental factors all might affect the immune reactivity of the newborn infant to bacteria and viruses. Biliary atresia (BA) is a disease that affects mainly neonatal infants, resulting in a high mortality in the absence of a liver transplantation.[1] The cause of BA remains unclear with immunologic, genetic, and maternal factors all suggested to potentially contribute to disease development. With the exception of surgery to remove the biliary blockage, advances in basic research and the clinical treatments have been hindered in part because of the failure of suitable animal models that mimic the characteristics of BA patients.

The mouse model of BA induced by inoculation with rhesus rotavirus (RRV) is currently used to investigate the development of acute bile duct damage in neonatal mice. Disease characteristics such as jaundice, destruction of the bile ducts by inflammatory cell infiltration are similar to

Supported by the Science and Technology Project of Guangzhou grant 201707010014 (R.Z.) and the National Natural Science Foundation of China grants 81600399 (R.Z.), 81770510 (R.Z.), and grant 81671498 (Y.C.).

R.Z., Z.L., and M.F. contributed equally to this work.

Disclosures: R.Z., Z.L., Y.C., and H.X. have submitted patent CN106172229B on the method for the establishment of chronic biliary atresia mouse model in China.

https://doi.org/10.1016/j.ajpath.2018.07.024

those observed in BA patients. With the use of this animal model, investigators have shown that components of both the innate and adaptive immune systems, such as natural killer cells, $CD4^+$ T cells, $CD8^+$ T cells, and B cells, contribute to tissue damage,[2–5] and direct or indirect targeting of the activity of these cell types has resulted in the rescue of the bile ducts and prolonged survival of the mice. However, additional cell types activated in the antiviral response may potentially play a role in the development and/or progression of disease in the RRV-induced BA model, and this possibility requires further investigation, especially because no obvious tissue fibrosis is observed and most mice died at days 12 to 16 after virus inoculation in this animal model.[6]

The granulocyte receptor-1 (Gr-1) molecule is a myeloid-derived cell surface marker initially found expressed in neutrophils. Depletion with an anti-Ly6G antibody reduced >90% of circulating neutrophils, increasing the susceptibility to protozoan *Toxoplasma gondii* infection.[7] However, expression of Gr-1 has now been demonstrated on other immune cells, such as plasmacytoid dendritic cells,[8] $CCR2^+$ inflammatory monocytes,[9] and myeloid-derived suppressor cells, which have been widely studied in cancer.[10,11] Therefore, $Gr\text{-}1^+$ cell depletion with an anti-Ly6G antibody not only reduced the number of neutrophils but also changed the responses induced by other immune cells. The role of the $Gr\text{-}1^+$ population has been investigated in various studies with the use of specific deleting antibodies, and the results have varied in terms of their effects on cytokine profiles and protection mediation. For example, no protection and no effect on cytokine production were observed in *Clostridium difficile*–induced colitis in mice.[12] There was a reduced clearance of high-dose recombinant *Mycobacterium bovis* bacilli Calmette-Guérin inoculation, but deletion of $Gr\text{-}1^+$ cells had no effect on low-dose recombinant *Mycobacterium bovis* bacilli Calmette-Guérin.[13] Reduced α-GalCer–induced antibacterial immunity and protection against *Listeria* monocytogenes infection in the liver have also been reported.[14] In virus infection studies in mice, it has been shown that $Gr\text{-}1^+$ cells, but not neutrophils, reduced herpes simplex virus type-1 replication and lesion development.[15] However, in Theiler's murine encephalomyelitis, a virus-induced demyelinating disease, the depletion of $GR\text{-}1^+$ cells increased virus-specific $CD4^+$ and $CD8^+$ T-cell responses and the expression of proinflammatory cytokines.[16] These apparent differences in the outcome of $GR\text{-}1^+$ cell depletion might relate to the type of immune response that is generated by the different pathogens, but it may also arise from the heterogeneity of the $Gr\text{-}1^+$ cell population. In neonatal mice, it has been shown that microbial colonization promoted prolonged dominance of $Gr\text{-}1^+$ cells and accelerated establishment of the $CD4^+$ T-cell populations in the spleen; however, the relationship between these two populations is not clear.[17]

Here, the role of $Gr\text{-}1^+$ cells were investigated in the RRV inoculation-induced mouse model of BA, but because Gr-1 is not found in humans, the comparable molecule CD177 was investigated in BA patients. Our data demonstrate the importance of the $Gr\text{-}1^+$ cell population, especially in chronic BA; therefore, $Gr\text{-}1^+$ cell population provides an appropriate animal model for the investigation of potential BA treatments.

Materials and Methods

Reagents and Antibodies

The antibody used for $Gr\text{-}1^+$ cell depletion was rat anti-mouse Ly6G (clone 1A8; Bio X Cell, West Lebanon, NH). The antibodies used for immunohistochemical staining were rat anti-mouse cytokeratin 19 (clone TROMA III; Developmental Studies Hybridoma Bank, Iowa City, IA), rat anti-mouse Gr-1 (BD Biosciences, San Jose, CA), rabbit polyclonal anti–tumor necrosis factor (TNF)-α (Abcam, San Francisco, CA). The rat anti-mouse polymorphonuclear leukocytes were from Upstate Biotechnology (Lake Placid, NY) and the rat anti-mouse F4/80 was obtained from R&D Systems (Minneapolis, MN). For flow cytometric analysis, all antibodies were purchased from eBioscience Inc. (San Diego, CA), including anti-mouse CD11b-fluorescein isothiocyanate, anti-mouse Gr-1–phycoerythrin/fluorescein isothiocyanate, anti-mouse Ly6G-phycoerythrin, anti-mouse Ly6C-peridinin chlorophyll protein-Cyanine5.5, anti-mouse CD4-peridinin chlorophyll protein-Cyanine5, anti-mouse CD3e-Alexa Fluor 488, anti-mouse CD8a-allophycoyanin, anti-mouse major histocompatibility complex-II–phycoerythrin, anti-mouse F4/80-allophycoyanin, and anti-mouse CD11c-phycoerythrin. For real-time PCR quantification, RNeasy Mini Kit was purchased from Qiagen (Hilden, Germany), the reverse transcription reagents were purchased from Invitrogen (Life Technologies Limited, N.T., Hong Kong), and Super Real PreMix was purchased from Tiangen Biotech Beijing Co., Ltd. (Beijing, China).

Mice

Day 12.5 pregnant BALB/c mice (aged between 10 and 12 weeks; weight, 35 to 40 g) were purchased from Guangdong Animal Experimental Center, maintained under specific pathogen-free conditions, housed in a 25°C room with a 12-hour dark–light cycle, and fed *ad libitum* autoclaved chow. Neonatal mice (average weight, 1.5 to 1.6 g) within the first 24 hours of birth were chosen for the mouse BA model. The experimental protocol was approved by The Institutional Animal Care and Use Committee of Sun Yat-Sen University Laboratory Animal Center (number IACUC-DB-16-0602) where all of the animal experiments were performed.

Experimental Design and the Administration of Anti-Ly6G Antibody

The RRV strain MMU 18006 was purchased from ATCC (Manassas, VA). The virus was amplified in MA104 cells, and the virus were quantified by a plaque assay method, as described previously.[18]

Neonatal mice were separated into three groups: the control group, the RRV group, and the RRV + anti-Ly6G group. The neonatal mice were injected with 20 μL of 1.5×10^6 PFU/mL RRV (RRV group) or supernatant of MA104 cell culture medium (control group) intraperitoneally within 24 hours of birth. For depletion of Gr-1$^+$ cells, the mice were pretreated with 5 μg of anti-Ly6G antibody per mouse by i.p. injection 4 hours before RRV injection, and then an additional injection of the antibody (10 μg/mouse) was given every 3 days until day 12 after RRV injection (Figure 1A). The mice that died within 5 days were excluded from further analysis. All mice were examined and recorded daily. The development of icterus on the skin not covered with fur and acholic stools that appeared on days 5 to 6 after injection indicated successful induction of BA. The animals were anesthetized and dissected under microscopy (SMZ1000; Nikon, Tokyo, Japan). The gross appearance of livers and bile ducts was photographed. Tissues were harvested and stored at −80°C for RNA/protein isolation or in 10% formalin for histologic sample preparation.

Histologic and Immunohistochemical Analysis

Mouse liver samples for immunostaining were fixed overnight in 10% formalin at room temperature for subsequent paraffin-embedding. Paraffin-embedded tissue

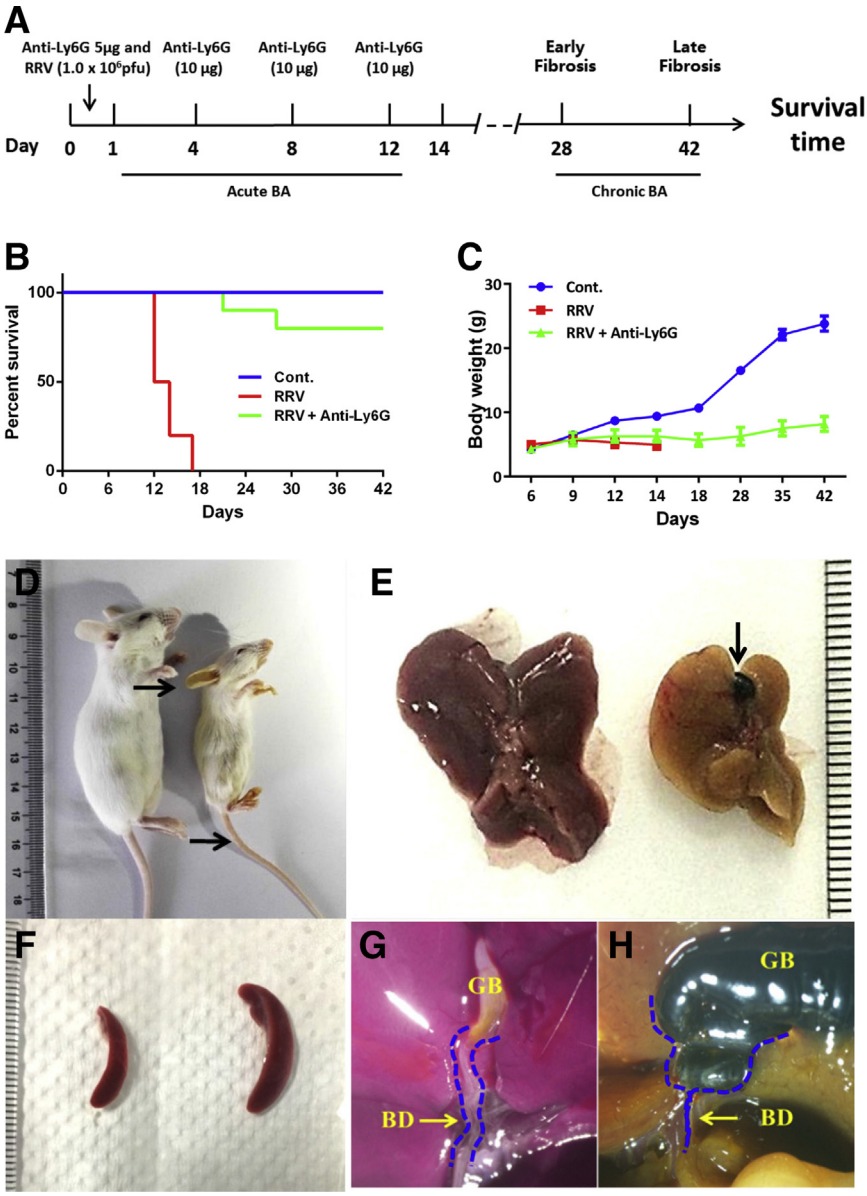

Figure 1 Effect of anti-Ly6G antibody on the rhesus rotavirus (RRV)-inoculated mouse biliary atresia (BA) model. **A:** Schematic representation showing low-dose anti-Ly6G antibody induction of mouse acute and chronic BA syndrome. The **Arrow** indicates the time of antibody and RRV injection within 24 hours after birth. **B:** Survival curve of anti-Ly6G antibody treatment. **C:** Body weight record for the control (Cont.), RRV-only, and RRV + Ly6G antibody groups until 42 days. **D:** Photograph of chronic BA mouse (right) at 42 days after RRV inoculation compared with a normal control mouse (left). The **arrows** indicate the jaundiced areas. **E:** Liver dissection comparing normal control mice (left) and chronic BA mice. The **arrow** indicates the enlarged gall bladder. **F:** Enlarged spleen of chronic BA (right) and normal control spleen (left). **G** and **H:** Comparison of the site of bile duct atresia in normal control mice (**G**) with chronic BA mice (**H**). **Dashed blue lines** indicate the border of the bile duct. $n = 10$ mice in each group (**B**). BD, bile duct; GB, gallbladder.

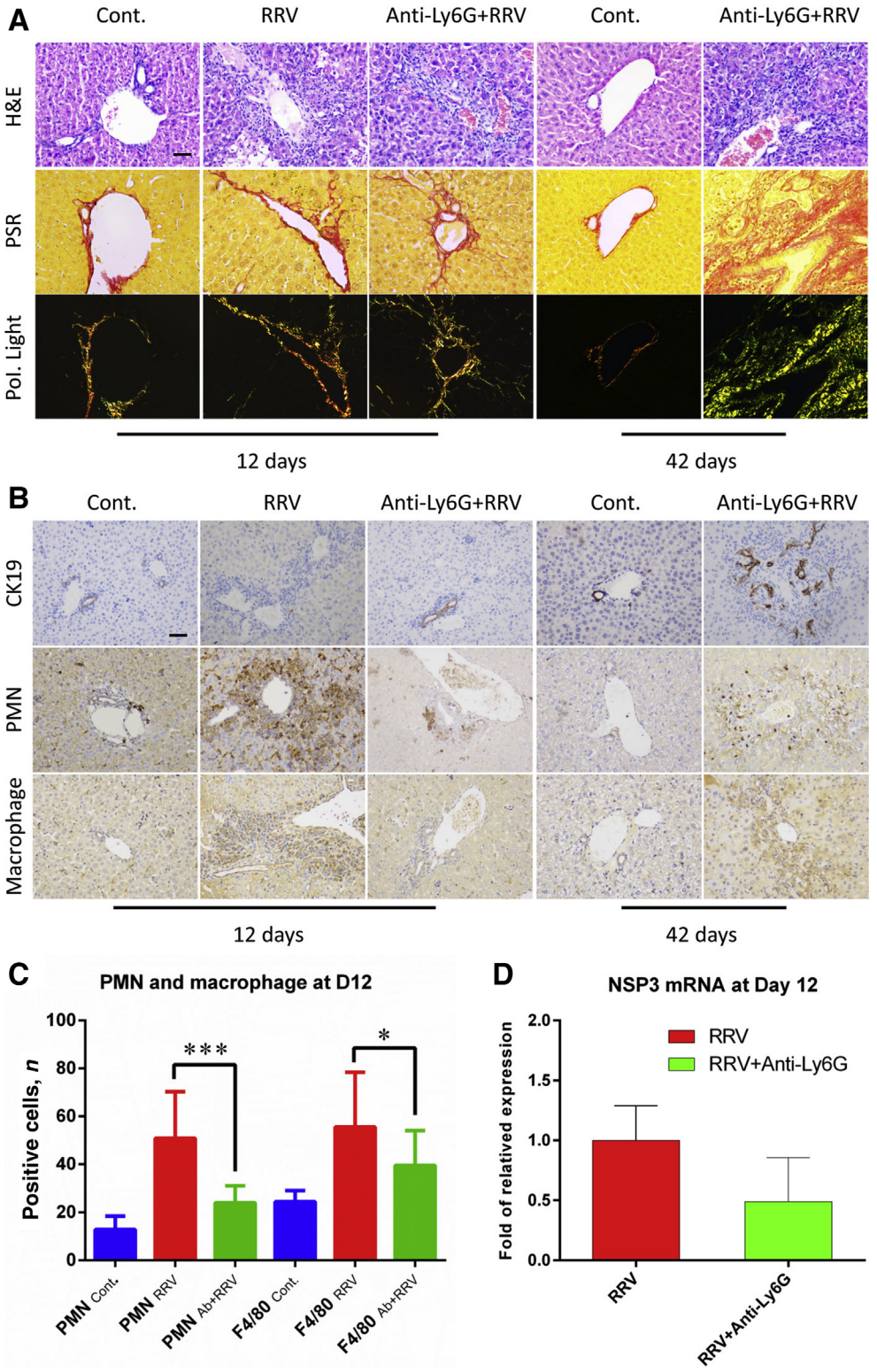

Figure 2 Liver tissue sections in normal control (Cont.) mice, rhesus rotavirus (RRV), and RRV + anti-Ly6G antibody (Ab) groups at day 12 and controls and RRV + anti-Ly6G at 42 days after RRV inoculation. **A:** Images of liver tissue sections showing histologic examination by using hematoxylin and eosin (H&E) staining. Collagen deposition illustrated by Picrosirius red staining (PSR). The sections were further observed by using polarized light microscopy (Pol. Light). **B:** Immunohistochemical staining showing the expression of biliary epithelial cells (CK19), and inflammatory cell infiltration of neutrophils (PMN) and macrophages in the different treatment groups. **C:** Comparison of the number of PMNs and macrophages in liver tissue sections. **D:** Real-time quantitative PCR results of RRV Nonstructural protein 3 (NSP3) expression comparing the RRV and RRV + anti-6G antibody groups at day 12 after virus inoculation. $n = 3$ to 5 samples in each group, at least five sections containing a portal vein were counted in each sample (**C**). $^{*}P < 0.05$, $^{***}P < 0.001$. Scale bars = 50 μm (**A** and **B**).

sections (4 μm thick) were dewaxed and rehydrated and then stained with hematoxylin and eosin for histologic analysis. For immunohistochemistry staining antigen retrieval was performed in a citrate buffer (10 mmol/L, 0.01% Tween20, pH 6.0) for CK19 or Tris-EDTA Buffer (10 mmol/L Tris Base, 1 mmol/L EDTA Solution, pH 9.0) for Gr-1. The removal of endogenous peroxidase was performed by 3% hydrogen peroxide treatment for 10 minutes. The sections were then incubated for 30 minutes in blocking solution (antibody diluent; Dako Denmark A/S, Glostrup Denmark), followed by overnight incubation at 4°C in blocking solution that contained the primary antibodies. Immunostaining was completed by using the Dako EnVision + system (Dako). The results were analyzed with a Nikon microscope and captured with NIS-Elements F4.0 (Nikon Instruments Inc., Melville, NY).

For detection of liver fibrosis, collagen was stained with Picrosirius red. After counterstaining with hematoxylin, the tissue section was treated with Picrosirius red for 1 hour at room temperature; the sections were then mounted and analyzed. Details of collagen deposition can be observed with polarized contrast light microscopy (Leica DMI8+DFC7000T; Leica Microsystems, Wetzlar, Germany), under which conditions immature collagen has a green color.[19]

Mononuclear Cell Isolation and Flow Cytometric Analysis

A single-cell suspension was isolated from the spleens by gently mincing the tissue and passing it through a 70-μm cell strainer and then centrifuging the cell suspension (270 × *g*, 4°C two times). The cells were resuspended in 30% Percoll (Sigma-Aldrich Corp, St. Louis, MO) and centrifuged at 400 × *g* at room temperature for 22 minutes, and then the red blood cells were lyzed by treatment with lysis buffer (Tiangen Biotech Beijing Co., Ltd.) for 5 minutes. The cell pellet was resuspended in RPMI 1640 medium (Invitrogen). Specific cell surface markers were used to perform cellular phenotyping by labeling with the appropriate antibodies. Flow cytometry was performed with a BD FACS Canto system (BD Biosciences, San Jose, CA) and analyzed with FlowJo software verison 10.0.7 (FlowJo LLC, Ashland, OR). Cell populations were selected according to forward/side scatter, gated according to isotype controls to account for background fluorescence, and subjected to secondary analysis based on fluorescence signals from specific antibodies.

Measurement of Clinical Biochemistry Variables

Mouse sera were collected at the end of the experiments and analyzed by the hospital's clinical laboratory by using a Hitachi Pre-Analytical Process Automation System with 7600 Clinical Analyzer (Hitachi, Tokyo, Japan). The 10 variables analyzed were as follows: alanine aminotransferase; aspartate aminotransferase; alkaline phosphatase; total protein; albumin; globulin; total bilirubin (TBIL); direct bilirubin (DBIL); indirect bilirubin (IBIL) and total bile acids.

Gene Expression Analysis with Quantitative PCR

For virus detection, liver RNA was extracted, and 1 μg of RNA was used for reverse transcription by using SuperScript III First-Strand Synthesis System (Thermo Fisher Scientific, Waltham, MA) according to the manufacturer's instructions. The real-time PCR-cyber green kit Fast SYBR Green Master Mix was used to detect the virus titer by determining the nonstructural gene *NSP3*. The primer sequence for *NSP3* was forward, 5′-TTGAAGAGAAAATGGAAGTAGATA-CAA-3′, and reverse, 5′-TACTTCTCATTAACCCGAT-GTTTCA-3′, and for TNF-α forward, 5′-TAGCTCCCA-GAAAAGCAAGC-3′, and reverse, 5′-TTTTCTGGAGG-GAGATGTGG-3′. PCR was performed with a C1000 Thermal Cycler (Bio-Rad Laboratories Co., Ltd., Hercules, CA).

Patients

Liver samples were taken with a wedge biopsy from 1− to 5−month-old infants undergoing intraoperative cholangiograms and Kasai operations at the time of diagnosis of BA at the hospital. The diagnosis was confirmed by histology of the liver and the portal plate that demonstrated bile duct obstruction. Liver samples from patients with choledochal cysts were used as the disease control. The human study protocols conformed to the ethical guidelines of the 1975 Declaration of Helsinki, and studies were approved by the Institutional Review Board of Guangzhou Women and Children's Medical Center, China. BA liver fibrosis grading followed the METAVIR score system (*https://www.uptodate.com/contents/histologic-scoring-systems-for-chronic-liver-disease*, subscription required).

Statistical Analysis

The data are presented as means ± SEM. The statistical analyses were performed by an unpaired two-tailed *t*-test by using GraphPad Prism software version 6.0 (GraphPad Software Inc., La Jolla, CA) with $P < 0.05$ indicating statistical significance.

Results

Amelioration of BA in RRV-Inoculated Mice by Anti-Ly6G Treatment

The mouse BA model was adapted from a previous well-characterized protocol in which neonatal mice were inoculated with the RRV virus within 24 hours after birth.[6] Compared with the RRV treatment, as a result of which

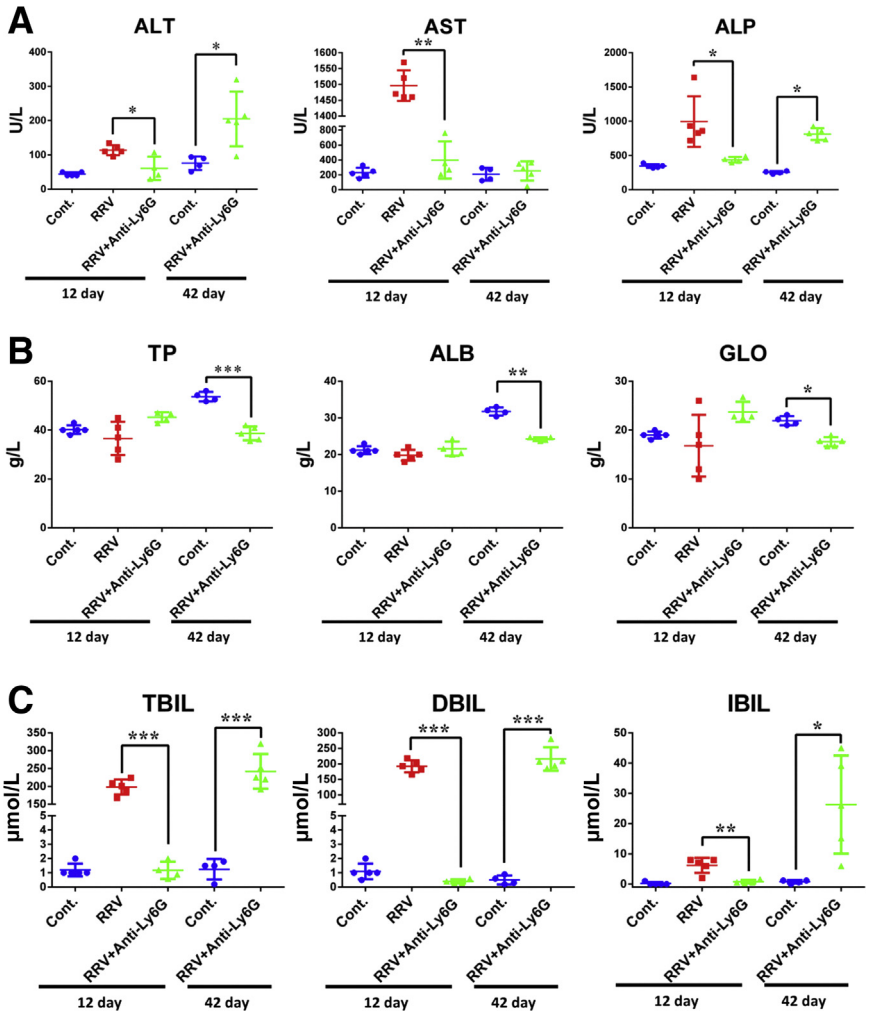

Figure 3 Clinical examination of liver function in the blood of mice comparing the effects of anti-Ly6G antibody in chronic phase biliary atresia (BA) in the rhesus rotavirus (RRV)+anti-Ly6G group. Blood was collected after the experiments and examined in the clinical laboratory of the hospital. **A:** Liver enzyme analysis. **B:** Serum protein levels analysis. **C:** Bilirubin metabolism analysis. The detailed values are shown in Supplemental Table S1. $n = 3$ to 5 mice in each group. $^{*}P < 0.05$, $^{**}P < 0.01$, and $^{***}P < 0.001$. ALB, albumin; ALP, alkaline phosphatase; ALT, alanine aminotransferase; AST, aspartate aminotransferase; Cont., control; DBIL, direct bilirubin; GLO, globulin; IBIL, indirect bilirubin; TBIL, total bilirubin; TP, total protein.

mice often died within 12 to 14 days, a high dose of anti-Ly6G antibody treatment (100 μg/mouse) totally prevented death, the body weights were the same as the control group, and there was no evidence of jaundice (Supplemental Figure S1).

Low Doses of Anti-Ly6G Antibody Treatment May Promote the Development of Chronic BA

Mice were given a reduced dosage of anti-Ly6G antibody that was repeated every 4 days (Figure 1A). In the RRV-only group the median survival time was 13 days; in contrast, most of the antibody-treated mice survived with only minor jaundice and no weight loss (Figure 1B). However, approximately 25% to 30% of mice had BA syndromes with persistent jaundice and lower body weights (8.19 ± 1.14 g versus 23.8 ± 1.17 g) but were able to survive for >42 days (Figure 1C and Supplemental Figure S2). Therefore, the anti-Ly6G treatment produced a *de novo* phenotype in the BA mouse, which was termed chronic BA, as opposed to its counterpart, acute BA. Time point samples were collected at days 21, 28, and 42, and staining tissue sections with Picrosirius red revealed a progressive increase in tissue fibrosis in the liver (Supplemental Figure S3).

Mice with chronic BA that survived for 42 days were collected for detailed analysis. Other than their small size, jaundice was apparent on the skin of the ear, foot, and tail (Figure 1D and Figure 2). The livers of these mice were dissected and compared with the control livers. They were reduced in size and pale yellow in color with an enlarged gallbladder filled with dark blue bile (Figure 1E). Enlarged spleens were present in chronic BA (Figure 1F) and in the portal areas of the livers compared with the normal bile duct (Figure 1G); moreover, atresia of a fragment of the bile ducts was also observed (Figure 1H).

Pathologic Changes in the Mouse BA Model in Response to Treatment with Low-Dose Anti-Ly6G Antibody

Analysis of liver tissue sections showed that treatment with low doses of anti-Ly6G reduced the portal tract inflammation

at day 12, and no tissue apoptosis was observed, unlike the RRV-alone group. However, cellular infiltration was still present in 42-day liver tissue sections (Figure 2A). In terms of liver fibrosis, Picrosirius red staining results demonstrated that at day 12 after RRV inoculation, there was a slight increase in collagen deposition in the portal triad. After treatment with the anti-Ly6G antibody there was no obvious change in collagen expression, but it was greatly increased at 42 days for the BA tissue samples (Figure 2A and Supplemental Figure S3). When viewed under a polarized contrast light microscope, it was observed that collagen fibers had penetrated into the nearby liver tissue. Large collagen deposition, mainly green in color, was observed in 42-day BA tissue samples (Figure 2A) and was further increased in mice kept for ≥49 days without an augmentation in body weight (Supplemental Figure S2). With the reduced inflammation in the portal triad, preserved CK19$^+$ bile ductules were observed at day 12; however, at day 42, mature bile ductules were difficult to detect, although an increase in CK19$^+$ cells could be observed (CK19) (Figure 2B). In terms of the extrahepatic bile duct in the chronic BA mouse, a serial dissection of the mouse liver in the portal area showed a blockade of the extrahepatic bile duct together with the infiltration of inflammatory cells (Supplemental Figure S4). Inflammatory cell infiltration was an important characteristic of acute BA. The number of both neutrophils and macrophages were greatly reduced at day 12 after anti-Ly6G administration ($P < 0.001$ in both polymorphonuclear leukocytes and $P < 0.05$ in macrophage; $n = 3$ in control, $n = 6$ in RRV-alone, and $n = 4$ in anti-Ly6G + RRV group) (Figure 2, B and C). Virus in liver tissue was also detected with real-time quantitative PCR by using RRV *NSP3* as a primer but was not significantly different compared with the RRV-alone group ($P = 0.0667$) (Figure 2D).

Liver Function Evaluated from Clinical Biochemistry Examination

Compared with RRV alone, at day 12 after RRV inoculation, the effect of low-dose anti-Ly6G antibody treatment reduced liver damage in terms of liver enzyme levels, such as alanine aminotransferase (104.40 ± 11.37 U/L versus 60.75 ± 17.67 U/L; $P < 0.05$), aspartate aminotransferase (1244.00 ± 135.76 U/L versus 339.50 ± 125.33 U/L; $P < 0.01$), and alkaline phosphatase (750.00 ± 126.89 U/L versus 439.75 ± 20.10 U/L; $P < 0.05$) in acute BA. For chronic BA, liver alanine aminotransferase and alkaline phosphatase were increased compared with the normal control group (both $P < 0.05$) (Figure 3A). For serum protein levels, no obvious changes were found in the acute phase of BA mice. A reduction of the serum protein levels was observed for total protein (53.68 ± 0.96 g/L versus 42.44 ± 1.23 g/L; $P < 0.001$), albumin (31.75 ± 0.55 g/L versus 24.26 ± 0.44 g/L; $P < 0.01$), and globulin (21.93 ± 0.46 g/L versus 17.62 ± 0.93 g/L; $P < 0.05$) compared with the normal control mice (Figure 3B). The most obvious changes were found in bilirubin levels because TBIL, DBIL, and IBIL levels in RRV + anti-Ly6G mice were reduced compared with RRV alone in acute BA ($P < 0.001$ for TBIL and DBIL; $P < 0.01$ for IBIL) (Figure 3C). In chronic BA, the levels of TBIL, DBIL, IBIL, and total bile acids were increased (242.0 ± 48.67 μmol/L versus 1.25 ± 0.17 μmol/L and 215.7 ± 37.71 μmol/L versus 0.5 ± 0.31 μmol/L) for total and direct bilirubin, respectively ($P < 0.001$ in TBIL, DBIL, and total bile acids; $P < 0.01$ in IBIL) (Figure 3C), which indicated greatly reduced liver function in the chronic phase of BA. The details of the biochemistry examination can be found in Supplemental Table S1.

Changes in Immune Cells in Acute and Chronic BA after Anti-Ly6G Antibody Treatment

With the use of flow cytometry, Gr-1$^+$, CD4$^+$, and CD8$^+$ T-cell populations at different time points of BA with and without anti-Ly6G treatment were examined (Figure 4). CD11b$^+$Gr-1^{hi} cells were expressed at high levels of approximately 30% in the spleen at birth but were sharply reduced to 3% by the first week and even lower than that at day 12. RRV inoculation reduced the Gr-1$^+$ cell population at day 3 to <5% ($P < 0.01$) which was restored to >10% at day 12 after virus inoculation ($P < 0.01$) compared with the control. Pretreatment with the anti-Ly6G antibody before virus inoculation greatly reduced the CD11b$^+$Gr-1^{hi} cell level to lower than 1% ($P < 0.001$ at day 1 and $P < 0.05$ at day 3) compared with the RRV-only group, but at day 12, although expression was lower, CD11b$^+$Gr-1^{hi} cells were still observed ($P < 0.01$) compared with the RRV-only group. Compared at day 42, the CD11b$^+$Gr-1^{hi} cell level was still higher than that of the control mice ($P < 0.05$) (Figure 4, A and B). For CD11b$^+$Gr-1^{int} cells, there was a reduction in their level from 5% to 2% in the first week after birth in the control mice. Compared with control mice, RRV treatment initially increased the cell population by 50%, reduced to lower than control levels at day 3 ($P < 0.01$), and then sharply increased fivefold until day 12 after virus inoculation ($P < 0.001$). Anti-Ly6G antibody treatment had no obvious effects on earlier time points, but at day 12, there was a 30% reduction in CD11b$^+$Gr-1^{int} cells ($P < 0.01$) (Figure 4, A and C).

CD4$^+$ T cells progressively increased after birth from 0.14% to 1.36% at day 12, indicating the establishment of adaptive immunity in the neonatal mice. Inoculation with RRV increased the CD4$^+$ T-cell population by twofold on days 3, 7, and 12 ($P < 0.001$, $P < 0.01$, and $P < 0.01$, respectively). Treatment with anti-Ly6G only slightly reduced the CD4$^+$ T cells, namely, at day 1 from 0.14% to 0.08% ($P < 0.01$) and at day 12 from 2.93% to 2.24% ($P < 0.05$) (Figure 4, D and E). Similar to CD4$^+$ T cells, the development of CD8$^+$ T cells was observed from day 1 but was greatly increased by day 12 after birth. Enhancement of CD8$^+$ T cells after RRV inoculation was marked by day 12

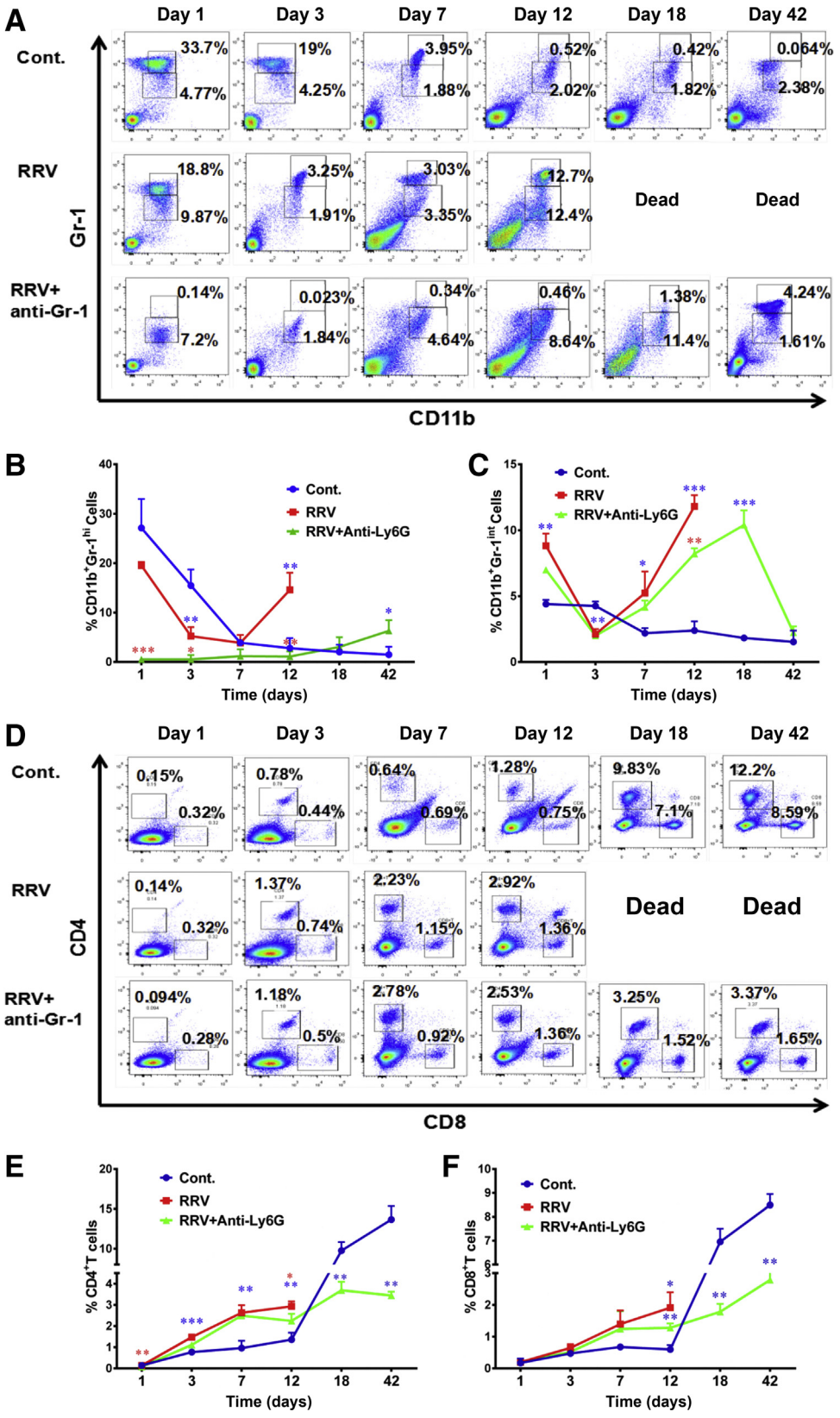

Figure 4 Flow cytometric analysis of immune cells in the spleen of the different treatment groups. The spleens were collected after the experiment, and the mononuclear cells were obtained and stained with the appropriate antibodies. **A** and **D:** Analysis of GR-1 and CD11 (**A**) and CD4 and CD8 (**D**) expression at different days after rhesus rotavirus (RRV) and RRV + anti-Gr-1 antibody treatment compared with a normal control (Cont.) group. **B**, **C**, **E**, and **F:** Graphs showing the expression of $CD11b^{+}Gr\text{-}1^{hi}$ (**B**), $CD11b^{+}Gr\text{-}1^{int}$ (**C**), $CD4^{+}$ (**E**), and $CD8^{+}$ (**F**) at different time points for the treatment groups. $n = 3$ to 5 spleens in each group. $^{*}P < 0.05$, $^{**}P < 0.01$, and $^{***}P < 0.001$ versus control.

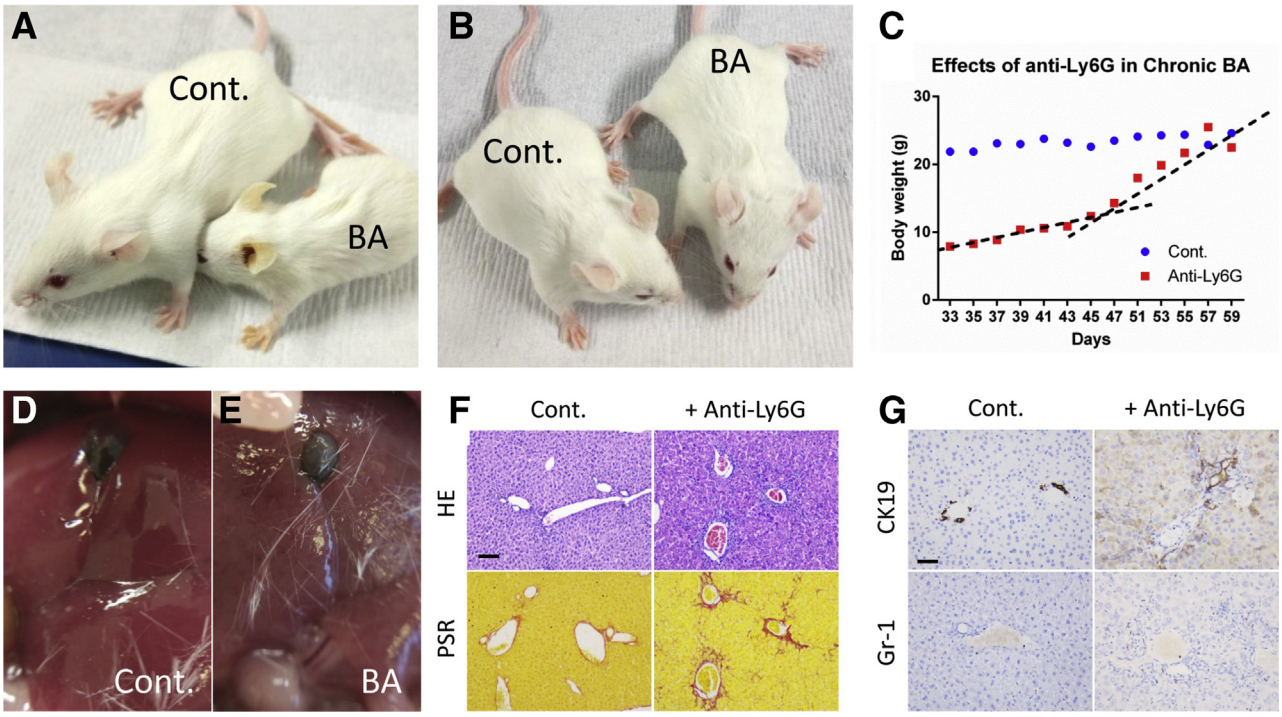

Figure 5 Therapeutic effects of anti-Ly6G antibody on the chronic mouse biliary atresia (BA) model. **A:** Chronic BA mice were given 100 μg of anti-Ly6G antibody by i.p. injection on day 28. **B:** The mice were examined and photographed at day 60. **C:** The body weights of mice with chronic BA and control (Cont.) mice were recorded and compared. The **black dashed lines** show the trends of body weight changes after anti-Ly6g antibody treatment. **D** and **E:** Livers of normal control (**D**) and chronic BA (**E**) mice treated with anti—Gr-1 antibody were dissected, photographed, and compared. **F:** Histologic analysis and tissue fibrosis shown by hematoxylin and eosin (HE) staining and Picrosirius red (PSR) staining. **G:** Intrahepatic ductular (CK19$^+$) detection in normal control and a chronic BA mouse treated with anti-Ly6G antibody compared with a normal control mouse. Liver Gr-1$^+$ cells were detected by using anti-Ly6G/Ly6C antibodies. Scale bars = 50 μm.

with a threefold increase. Although the anti-Ly6G antibody—treated group showed a trend of reduced up-regulation of CD8$^+$ T cells, it was not statistically significant (Figure 4, D and F).

Effect of Anti-Ly6G Antibody Treatment in the Chronic Phase of Disease in the Mouse BA Model

Because Gr-1$^+$ cells are still present in the chronic phase of the mouse BA model, the mice were administered the anti-Ly6G antibody as a single high dose (100 μg/mouse) at day 28 ($n = 3$) (Figure 5A). The results demonstrated the beneficial effects on the general health of the mice such as recovery from both jaundice observed in skin (Figure 5B) and body weight loss with similar body weights of approximately 20.0 g (Figure 5C). However, compared with normal livers (Figure 5D), dissection of the treated BA liver revealed that it still had a rough surface which suggested that the mice had not fully recovered to control levels (Figure 5E). Liver tissue sections had reduced cellular infiltration (Figure 5F) but tissue fibrosis was still present (Figure 5F), although less pronounced than that of mice receiving no treatment (Supplemental Figure S4). In the bile ductules (CK19$^+$), the presence of tube-like structures could be observed (Figure 5G), and Ly6G$^+$ cells could still be detected in the tissue sections compared with that of the control tissues (28.92 ± 15.77 high-power field versus 1.22 ± 2.22 high-power field) (Figure 5G).

Comparison of Mouse BA Model with Human BA Patient Samples

BA is a progressive inflammation and pathologic process leading to fibrosis. However, in the RRV-inoculated mouse BA model only the acute phase, which mainly presented as inflammation, could be observed.[6] In the anti-Ly6G + RRV mouse BA model described here, both the acute and chronic phases could be observed. In the acute phase, there was inflammatory cell infiltration without major tissue fibrosis (Figure 6A), and, in the later chronic phase, a large amount of tissue fibrosis was observed, as illustrated by Picrosirius red staining (Figure 6B), which corresponded at least in part to the pathology of BA patient samples and thus provided an animal model that could be investigated in parallel with human BA studies. It has been suggested that the molecule homologous to Ly6G in humans was CD177,[20] and CD177 expression in human BA patient samples was detected by immunohistochemical methods. The results revealed the presence of CD177 cells in both the cellular infiltration phase and the fibrotic phase of the disease ($P < 0.001$; $n = 6$ in choledochal cysts and $n = 5$ each in BA early or late stage) (Figure 6, C and D) which was similar to the

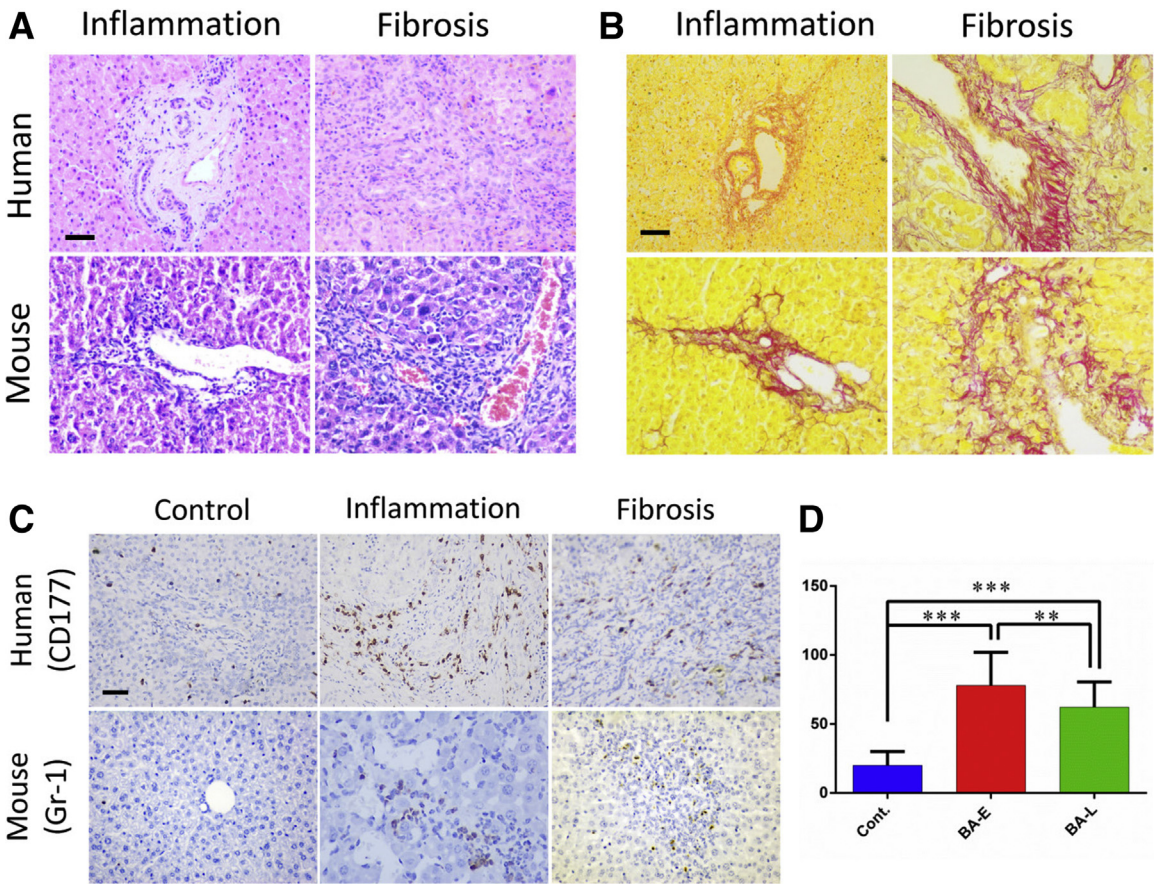

Figure 6 Comparison of tissue sections between the mouse biliary atresia (BA) model and human BA tissue sections. Human BA samples with mostly inflammation and tissue fibrosis were selected and compared with the mouse model of both acute BA and chronic BA. **A:** Histologic analysis with hematoxylin and eosin (H&E) staining. **B:** Tissue fibrosis analysis with Picrosirius red staining. **C:** Immunohistochemistry staining with CD177 in human BA tissue sections and anti–Gr-1 in mouse BA model liver sections comparing inflammation and liver fibrosis. **D:** CD177 number was counted and compared with disease control (Cont.) mice (choledochal cysts), $n = 6$ mice in control group; $n = 5$ mice each in early and late BA. $^{**}P < 0.01$, $^{***}P < 0.001$. Scale bars = 50 μm.

mouse model, suggesting that $CD177^+$ cells may play an important role in the disease process of human BA. Myeloperoxidase (MPO) was abundant in neutrophils, monocytes, and macrophages, which played a role in tissue damage; colocalization with $CD177^+$ cells was determined by double immunohistochemistry staining. A portion of the $CD177^+$ cell population was MPO^+, whereas others were not. This latter population was dominant in the control group (choledochal cysts) where only a few $CD177^+$ cells and nearly no MPO^+ cells were present.

Discussion

In this study, with the use of an anti-Ly6G antibody to deplete or reduce $CD11b^+Gr\text{-}1^+$ cells in RRV-inoculated mouse BA atresia model, an amelioration of acute BA syndrome and prolonged survival rates were achieved. Administration of a reduced dosage of the antibody produced the chronic BA with tissue fibrosis, which further indicated that the number of $Gr\text{-}1^+$ cells had altered the disease outcome in the acute and chronic stages. Furthermore, the presence of $Gr\text{-}1^+$ cells in tissue fibrosis and the observation that the depletion of these cells favored recovery is an indication that the $Gr\text{-}1^+$ cells may play a central role in the process of BA pathogenesis in this experimental model. The existence of CD177, which is a homolog of Ly6G, in human BA implies that $Gr\text{-}1^+$ cells may have a deleterious role in the development of BA in humans.

The function of $Gr\text{-}1^+$ cells in BA has not been reported previously. By using an anti–Gr-1 monoclonal antibody, RB6-8C5 in the RRV-inoculated mouse acute BA model, our preliminary studies found no obvious beneficial effects on the rescue of RRV-inoculated mice from death (data not shown). It has been shown that RB6-8C5 can deplete $CD11b^+Gr\text{-}1^+$ cells in the spleen and peripheral blood but not in the liver of mice with tumors.[21] In RRV-induced BA, tissue damage mostly occurred in the liver portal triad, which can partially explain the syndrome. Furthermore, studies in adult mice indicated that depletion by RB6-8C5 not only deletes neutrophils but all $Gr\text{-}1^+$ cells compared with the use of anti-Ly6G which mostly targets neutrophils and greatly increases levels of TNF-α in response to

lipopolysaccharide stimulation.[22] TNF-α is suggested to be a key factor in epithelial cell damage[23] in both BA patients and in the mouse model mediated through the TNF-α receptor TNFR2. In this study, real-time quantitative PCR showed expression of TNF-α mRNA in the RRV group but not in the antibody-treated group, and immunohistochemical staining indicated that expression was mostly found in inflammatory cells (Supplemental Figure S5), suggesting that ameliorated tissue damage may occur as a consequence of reducing inflammation.

In this study, the Gr-1$^+$ cell population was separated into CD11b$^+$Gr-1^{hi} and CD11b$^+$Gr-1^{int} by their different characteristics such as number of granules, level of Gr-1 expression, myeloid and granulocyte marker expression profiles, and nuclear shape. Lee et al[24] classified CD11b$^+$Gr-1^{hi} cells as neutrophils and the CD11b$^+$Gr-1^{int} cells as monocytes. Anti-Ly6G antibody depletion of Gr-1$^+$ cells mostly targets CD11b$^+$Gr-1^{hi} cells but is less effective on the CD11b$^+$Gr-1^{int} cell population, which appears only at day 12 after virus inoculation when a reduction in the former population of cells is observed. For CD11b$^+$Gr-1^{hi} cells, our results are in agreement but with slight differences to those of Daley et al[22] because they reported no effect on the depletion of monocytes or CD11b$^+$Gr-1^{int} cells in the mouse. In their experiments they administered only a single injection, and the different outcomes observed on day 12 on CD11b$^+$Gr-1^{int} cells might be due to a cumulative effect of the antibody on the monocytes. Evaluation of liver neutrophil and macrophage numbers further confirmed the reduction of the infiltrating inflammatory cells. Together with the possible reduction of TNF-α expression, our results suggest the anti-Ly6G antibody administration reduces inflammation in the portal triad, partially preserves the bile ducts, and prevents mouse death by acute BA.

Although the reduction of the inflammatory cells rescued the mice from death, the reduction of immunity also diminished the antiviral activity, as a result of which RRV levels at day 12 were similar to those in the RRV-alone group. The numbers of CD4$^+$ and CD8$^+$ T cells in control mice were relatively low at the time of birth and increased progressively from day 12. Viral infection augmented the number of T cells, both CD4$^+$ and CD8$^+$ populations, suggesting that they may contribute to the pathologic process in acute BA. The anti-Ly6G antibody had no effects on T-cell numbers compared with RRV-alone treatment. However, the number of T cells still remained low on day 18, implying that adaptive immunity was restricted and confirming that the interaction between neutrophils and T cells is essential for the activation and function of both innate and adaptive immunity.[25] The reduction in Gr-1 cells, including neutrophils, affects T-cell development and its antiviral function. The persistent presence of a virus causes chronic inflammation, which was observed in this model of BA. However, only 20% to 30% of mice developed chronic BA, suggesting that other factors might contribute to the disease process.

The presence of Gr-1$^+$ cells in our chronic BA model suggested that the function of these cells might be to promote the tissue fibrosis, especially because depletion of these cells with anti-Ly6G antibody improved the general condition of the BA mice. However, collagen deposition was still present; therefore, more time might be required to achieve a more complete disease resolution. Few studies have addressed the role of Gr-1$^+$ cells; however, in some animal models, Gr-1$^+$ macrophages,[26] Gr-1$^+$ neutrophils,[27] Gr-1$^+$ myeloid cells,[28] and Gr-1$^+$ granulocytes have been reported to enhance fibrosis.[29] However, the function of neutrophils in tissue fibrosis is not well established, although in the lungs there is evidence that neutrophil elastase promotes the differentiation of myofibroblasts.[30] Administration of the anti-Ly6G antibody reduced the number of neutrophils in acute BA, but treatment was only applied until day 12 after RRV inoculation. In the chronic phase, neutrophils can still accumulate and promote tissue fibrosis in the portal triad. Taken together with features of the BA syndrome such as jaundice, low body weight, and elevated TBIL, DBIL, and alkaline phosphatase compared with the control mice, these observations imply that the chronic BA disease model is similar to that of human BA. Our results show that depletion of Gr-1$^+$ cells in chronic BA ameliorates the symptoms of the condition and indicate that neutrophils play a key role in this disease. However, details on the mode of action, such as potential interactions with other immune cells and myofibroblasts in BA, still need further research.

Expression of CD177 in BA patients has not been reported previously. A study that used knockout mice indicated the CD177$^+$ cells produced high levels of transforming growth factor-β and neutrophil extracellular traps,[31] which are strong activators of tissue fibrosis, suggesting that an increase in CD177$^+$ cells might promote tissue fibrosis in human patients. CD177 in humans is partly expressed on neutrophils, and this was confirmed by double staining for CD177 and human neutrophil-specific antibody anti-MPO (Supplemental Figure S6), which indicated at least three types of cells present in BA patients (CD177$^+$MPO$^+$, CD177$^-$MPO$^+$, and CD177$^+$MPO$^-$); the relationship of these cells to BA is still under investigation and requires a larger sample size. This finding, taken together with our anti-Ly6G antibody findings that BA syndrome is reduced when an antibody is administered at the initiation time of chronic BA (at 42 days after virus inoculation), suggests that targeting CD177 cells may have therapeutic potential in the treatment of liver fibrosis in BA patients.

Acknowledgments

We thank the Department of Pathology and Biobank at the Guangzhou Women and Children's Medical Center for providing the clinical samples.

Supplemental Data

Supplemental material for this article can be found at *https://doi.org/10.1016/j.ajpath.2018.07.024*.

References

1. Gallo A, Esquivel CO: Current options for management of biliary atresia. Pediatr Transplant 2013, 17:95–98
2. Guo C, Zhu J, Pu CL, Deng YH, Zhang MM: Combinatory effects of hepatic CD8+ and NK lymphocytes in bile duct injury from biliary atresia. Pediatr Res 2012, 71:638–644
3. Shivakumar P, Sabla GE, Whitington P, Chougnet CA, Bezerra JA: Neonatal NK cells target the mouse duct epithelium via Nkg2d and drive tissue-specific injury in experimental biliary atresia. J Clin Invest 2009, 119:2281–2290
4. Mack CL, Falta MT, Sullivan AK, Karrer F, Sokol RJ, Freed BM, Fontenot AP: Oligoclonal expansions of CD4+ and CD8+ T-cells in the target organ of patients with biliary atresia. Gastroenterology 2007, 133:278–287
5. Mack CL, Tucker RM, Sokol RJ, Kotzin BL: Armed CD4+ Th1 effector cells and activated macrophages participate in bile duct injury in murine biliary atresia. Clin Immunol 2005, 115:200–209
6. Petersen C: Biliary atresia: the animal models. Semin Pediatr Surg 2012, 21:185–191
7. Egan CE, Sukhumavasi W, Bierly AL, Denkers EY: Understanding the multiple functions of Gr-1(+) cell subpopulations during microbial infection. Immunol Res 2008, 40:35–48
8. Nakano H, Yanagita M, Gunn MD: CD11c(+)B220(+)Gr-1(+) cells in mouse lymph nodes and spleen display characteristics of plasmacytoid dendritic cells. J Exp Med 2001, 194:1171–1178
9. Bruhl H, Cihak J, Plachy J, Kunz-Schughart L, Niedermeier M, Denzel A, Rodriguez Gomez M, Talke Y, Luckow B, Stangassinger M, Mack M: Targeting of Gr-1+,CCR2+ monocytes in collagen-induced arthritis. Arthritis Rheum 2007, 56:2975–2985
10. Suzuki E, Kapoor V, Jassar AS, Kaiser LR, Albelda SM: Gemcitabine selectively eliminates splenic Gr-1+/CD11b+ myeloid suppressor cells in tumor-bearing animals and enhances antitumor immune activity. Clin Cancer Res 2005, 11:6713–6721
11. Bronte V, Brandau S, Chen SH, Colombo MP, Frey AB, Greten TF, Mandruzzato S, Murray PJ, Ochoa A, Ostrand-Rosenberg S, Rodriguez PC, Sica A, Umansky V, Vonderheide RH, Gabrilovich DI: Recommendations for myeloid-derived suppressor cell nomenclature and characterization standards. Nat Commun 2016, 7:12150
12. McDermott AJ, Higdon KE, Muraglia R, Erb-Downward JR, Falkowski NR, McDonald RA, Young VB, Huffnagle GB: The role of Gr-1(+) cells and tumour necrosis factor-alpha signalling during Clostridium difficile colitis in mice. Immunology 2015, 144: 704–716
13. Panas MW, Letvin NL: Role for Gr-1+ cells in the control of high-dose Mycobacterium bovis recombinant BCG. Clin Vaccine Immunol 2014, 21:1120–1127
14. Emoto M, Emoto Y, Yoshizawa I, Kita E, Shimizu T, Hurwitz R, Brinkmann V, Kaufmann SH: Alpha-GalCer ameliorates listeriosis by accelerating infiltration of Gr-1+ cells into the liver. Eur J Immunol 2010, 40:1328–1341
15. Wojtasiak M, Pickett DL, Tate MD, Bedoui S, Job ER, Whitney PG, Brooks AG, Reading PC: Gr-1+ cells, but not neutrophils, limit virus replication and lesion development following flank infection of mice with herpes simplex virus type-1. Virology 2010, 407:143–151
16. Bowen JL, Olson JK: Innate immune CD11b+Gr-1+ cells, suppressor cells, affect the immune response during Theiler's virus-induced demyelinating disease. J Immunol 2009, 183:6971–6980
17. Kristensen MB, Metzdorff SB, Bergstrom A, Damlund DS, Fink LN, Licht TR, Frokiaer H: Neonatal microbial colonization in mice promotes prolonged dominance of CD11b(+)Gr-1(+) cells and accelerated establishment of the CD4(+) T cell population in the spleen. Immun Inflamm Dis 2015, 3:309–320
18. Arnold M, Patton JT, McDonald SM: Culturing, storage, and quantification of rotaviruses. Curr Protoc Microbiol 2009, Chapter 15:Unit 15C.3
19. Rich L, Whittaker P: Collagen and picrosirius red staining: a polarized light assessment of fibrillar hue and spatial distribution. Braz J Morphol Sci 2005, 22:97–104
20. Wang J-X, Bair AM, King SL, Shnayder R, Huang Y-F, Shieh C-C, Soberman RJ, Fuhlbrigge RC, Nigrovic PA: Ly6G ligation blocks recruitment of neutrophils via a beta2-integrin–dependent mechanism. Blood 2012, 120:1489–1498
21. Ma C, Kapanadze T, Gamrekelashvili J, Manns MP, Korangy F, Greten TF: Anti-Gr-1 antibody depletion fails to eliminate hepatic myeloid-derived suppressor cells in tumor-bearing mice. J Leukoc Biol 2012, 92:1199–1206
22. Daley JM, Thomay AA, Connolly MD, Reichner JS, Albina JE: Use of Ly6G-specific monoclonal antibody to deplete neutrophils in mice. J Leukoc Biol 2008, 83:64–70
23. Shivakumar P, Mizuochi T, Mourya R, Gutta S, Yang L, Luo Z, Bezerra JA: Preferential TNFalpha signaling via TNFR2 regulates epithelial injury and duct obstruction in experimental biliary atresia. JCI Insight 2017, 2:e88747
24. Lee S-C, Ju S-A, Sung B-H, Heo S-K, Cho HR, Lee EA, Kim JD, Lee IH, Park S-M, Nguyen QT, Suh QT, Kim BS: Stimulation of the molecule 4-1BB enhances host defense against Listeria monocytogenes infection in mice by inducing rapid infiltration and activation of neutrophils and monocytes. Infect Immun 2009, 77:2168–2176
25. Mantovani A, Cassatella MA, Costantini C, Jaillon S: Neutrophils in the activation and regulation of innate and adaptive immunity. Nat Rev Immunol 2011, 11:519–531
26. Engel DR, Krause TA, Snelgrove SL, Thiebes S, Hickey MJ, Boor P, Kitching AR, Kurts C: CX3CR1 reduces kidney fibrosis by inhibiting local proliferation of profibrotic macrophages. J Immunol 2015, 194:1628–1638
27. Liang M, Lv J, Zou L, Yang W, Xiong Y, Chen X, Guan M, He R, Zou H: A modified murine model of systemic sclerosis: bleomycin given by pump infusion induced skin and pulmonary inflammation and fibrosis. Lab Invest 2015, 95:342–350
28. Chen Y, Huang Y, Reiberger T, Duyverman AM, Huang P, Samuel R, Hiddingh L, Roberge S, Koppel C, Lauwers GY, Zhu AX, Jain RK, Duda DG: Differential effects of sorafenib on liver versus tumor fibrosis mediated by stromal-derived factor 1 alpha/C-X-C receptor type 4 axis and myeloid differentiation antigen-positive myeloid cell infiltration in mice. Hepatology 2014, 59:1435–1447
29. Tomasson MH, Sternberg DW, Williams IR, Carroll M, Cain D, Aster JC, Ilaria RL Jr, Van Etten RA, Gilliland DG: Fatal myeloproliferation, induced in mice by TEL/PDGFbetaR expression, depends on PDGFbetaR tyrosines 579/581. J Clin Invest 2000, 105: 423–432
30. Gregory AD, Kliment CR, Metz HE, Kim KH, Kargl J, Agostini BA, Crum LT, Oczypok EA, Oury TA, Houghton AM: Neutrophil elastase promotes myofibroblast differentiation in lung fibrosis. J Leukoc Biol 2015, 98:143–152
31. Zhou G, Yu L, Fang L, Yang W, Yu T, Miao Y, Chen M, Wu K, Chen F, Cong Y, Liu Z: CD177+ neutrophils as functionally activated neutrophils negatively regulate IBD. Gut 2018, 67:1052–1063